Engineering in Life Sciences
Eng. Life Sci. 2017, 17, 732–738
www.els-journal.com

Madalena Martins[1]
Nuno G. Azoia[1]
Manuel Melle-Franco[2]
Artur Ribeiro[1]
Artur Cavaco-Paulo[1]

[1]Centre of Biological Engineering (CEB), University of Minho, Campus of Gualtar, Braga, Portugal

[2]CICECO—Aveiro Institute of Materials, University of Aveiro, Campus Universitário de Santiago, Aveiro, Portugal

Research Article

Permeation of skin with (C_{60}) fullerene dispersions

Dispersions in transcutol/isopropyl myristate make C_{60} fullerene molecules suitable for transdermal delivery. We found that C_{60} can successfully permeate the skin using pig skin in Franz diffusion cells. Molecular dynamics simulations and transmission electron microscopy confirmed these observations. Basic cosmetic formulations with transcutol/isopropyl myristate without harsh organic solvents show a high potential for delivery of C_{60} for biopharmaceutical and cosmetics applications.

Keywords: Cosmetics / Delivery / Dispersion / Fullerene C_{60} / Transdermal

Received: November 24, 2016; *revised:* January 5, 2017; *accepted:* January 20, 2017

DOI: 10.1002/elsc.201600244

1 Introduction

Fullerenes are hydrophobic molecules composed of carbon atoms arranged in a spherical geometry with a hollow interior. In fullerenes, carbon atoms are typically interconnected by alternating length bonds. Thus, presents sp^2 carbon atoms hybridization arranged in hexagons and pentagons [1]. Fullerenes have attracted much attention of researchers from the discovery of their potential as a potent antioxidant [2–4]. Fullerenes are capable of scavenging free radicals including reactive oxygen and nitrogen species [5, 6]. These reactive species are generated in cells, and their presence induces cellular instability that leads to damage and ultimately cell death. Antioxidants are molecules able to perform the elimination or neutralization of free radical electrons. The benefits of antioxidants have been extensively investigated, particularly in general heath (e.g. extending the lifespan) or in skin aging (delaying the normal aging process) [7, 8].

Fullerene C_{60} can exhibit antioxidant functionality as it readily reacts with many free radicals deactivating them effectively. The discovery of this buckminsterfullerene, a stable and very symmetrical structure (carbon cluster) with 60 atoms, opened up an innovative way to treat a wide range of pathologies and diseases [9]. This include, radiation exposure [10], degenerative process related with skin aging [11], degenerative diseases (Parkinson's, Alzheimer's, multiple sclerosis) [12,13], osteoporosis [14], and, in general, inflammatory processes [15]. However, potential applications ranging from cosmetic/pharmaceutical to medical treatments have been impaired due to the fact that C_{60} is insoluble in water and polar solvents. Several solvents have been explored to solubilize fullerene C_{60} [16–19]. The toxicity of C_{60} fullerene is dependent of its structure, composition, and morphology [20]. The generalization about C_{60} fullerene toxicity it is ambiguous because it is dependent of several factors, such as, dose and time-dependent, functional groups in the case of functionalization, method of administration among others [21]. Therefore, future toxicological studies will be crucial for safety and effective methodologies.

To overcome the water solubility problem of C_{60} different biocompatible approaches is required. Fullerene derivatives have been developed for instance by covalent functionalization with hydrophilic chemical groups or by the encapsulation into supramolecular complexes such as cyclodextrin or polyvinylpyrrolidone [22, 23]. Further research demonstrated the solubility of fullerene C_{60} in fatty acids [24, 25] that allowed the possibility to use fatty acid esters of glycerol or others, for the delivery of fullerene and fullerene derivatives in living organisms [26]. Based on this, we developed herein dispersions of fullerene C_{60} in fatty acids suitable for transdermal application. As far as we know there is no cosmetic/pharmaceutical formulation available using fullerene C_{60} in isopropyl myristate and/or transcutol. These dispersions make fullerene C_{60} suitable to be delivered transdermally by direct application in the skin without harsh organic solvents or any chemical modification or encapsulation process.

2 Materials and methods

2.1 Materials

Fullerene C_{60} (purity: 99.5%) and isopropyl myristate (IPM) were purchased from Sigma-Aldrich (Spain). Transcutol (TRC) (diethylene glycol monoethyl ether) was kindly provided from Gattefossé Corporation (France). The skin permeation study was performed using pig skin that was kindly supplied by a slaughterhouse (Matadouro Central de Entre Douro e Minho,

Correspondence: Dr. Artur Cavaco-Paulo (artur@deb.uminho.pt), Centre of Biological Engineering, University of Minho, 4710-057 Braga, Portugal

Abbreviations: IPM, isopropyl myristate; **LLE**, liquid–liquid extraction; **TEM**, transmission electron microscopy; **TRC**, transcutol

Figure 1. Visual illustration of fullerene C_{60} dispersions (0.8 mg/mL) in IPM (left), in IPM with Transcutol (20% TRC) (center) and in water (right).

Portugal). All reagents were used as received without further purification.

2.2 Preparation method of fullerene C_{60} dispersions

The preparation of the fullerene C_{60} dispersions were as follows. The solid fullerene C_{60} was dispersed in water, in IPM and in IPM with 20% transcutol to a final concentration of 0.8 mg/mL of C_{60} for all solutions. The dispersions were vigorously stirred for 3 h at a room temperature with a magnetic stirrer.

2.3 In vitro permeation studies

The permeation profile was undertaken on a Franz diffusion cell (V-Series Franz Cells, PermeGear, USA). This apparatus consists of three cells, each one with a donor and receptor compartment. The pig skin specimen was mounted between the donor and receptor compartments, and 300 μL of the dispersion solution of C_{60} was placed on the top of the skin surface in the donor compartment. The receptor compartment was filled with 5 mL of 0.01 M phosphate buffered saline (pH 7.4) that was continuously stirred. The receptor liquid was maintained at 37°C using a circulating water bath for 24 h. A control sample was run in parallel with each assay.

The quantification of C_{60} in the receptor and donor compartments was determined by a simple liquid–liquid extraction (LLE) method. The experiments were carried out by mixing equal volumes of aqueous and organic (toluene) phases (5 mL). After extraction from the sample solution fullerene C_{60} was quantified by UV-vis spectroscopy.

2.4 Transmission electron spectroscopy

To visualize the C_{60} dispersions morphology into the skin, the samples were fixed with 2.5% glutaraldehyde and 2% paraformaldehyde in cacodylate buffer 0.1 M (pH 7.4). After post fixed in 2% osmium tetroxide in the same buffer, the samples were dehydrated with ethanol, carefully cut off, and embedded in Epon resin. Ultrathin sections (40–60 nm thickness) were prepared on a RMC Ultramicrotome (PowerTome, USA) using diamond knives (DDK, Wilmington, DE, USA). The sections were mounted on 200 mesh copper or nickel grids, stained with uranyl acetate and lead citrate for 5 min each, and examined under a JEOL JEM 1400 TEM (Tokyo, Japan). Images were digitally recorded using a CCD digital camera Orious 1100 W Tokyo, Japan.

2.5 Molecular dynamics simulations

The simulations were performed with GROMACS 4.6 [27] package using Martini force field [28]. The system size was chosen according to the minimum image convention taking into account a cut-off of 1.2 nm. The bonds lengths were constrained with LINCS [29]. Nonbonded interactions were calculated using a twin-range method, with short and long range cut-offs of 0.9 and 1.2 nm, respectively. Neighbor searching was carried out up to 1.2 nm and updated every ten steps. A time step of integration of 20 fs was used. A reaction field correction for the electrostatic interactions was applied using a dielectric constant of 15. Pressure control was implemented using the Berendsen barostat [30], with a reference pressure of 1 bar, 3.0 ps of relaxation time and isothermal compressibility of 3.0×10^{-5} bar^{-1}. Temperature control was set using the Berendsen thermostat [30] at 300 K. Each component of the system was included in separated heat bath, with temperatures coupling constants of 0.30 ps. The lipid membrane was built using the same approach described in our previous work [31]. The membranes are composed by ceramid-2, lignoceric acid, cholesterol, and cholesterol sulphate. The stratum corneum is composed by repeating units of double bilayers of this lipids. The separation between bilayers is around 5 Å, and the separation between the repeating double bilayers is typically 25 Å.

In all cases, the fullerene molecules were positioned randomly in water at the beginning of the simulations. The total simulation time, after the initial 20 ns of equilibration, was 1 μs for each simulation. For the simulations with several fullerene molecules the same conditions were applied. The objective is to demonstrate the behavior of the system under different concentrations of fullerene molecules. The number of added fullerene molecules has no direct correlation with experimental concentration.

In addition, a pulling simulation was performed for the fullerene molecule crossing the membrane, in order to calculate the potential of mean force of the process. For this, after an equilibration step of 20 ns, a 20 ns simulation with a pull rate of 0.3 nm/ns and a pull force constant of 1000 kJ/(mol nm^2) was run.

3 Results and discussion

The method used to prepare C_{60} dispersions was throughout a single phase mixture. Fullerene C_{60} at a concentration of 0.8 mg/mL was mixed in three different solutions: in IPM, in IPM with 20% TRC and in water. The samples were stirred until forming a uniform solution. Fullerene C_{60} dispersed in IPM and in IPM with TRC, but did not disperse in water as pristine fullerenes are insoluble in water. Dispersions showed a characteristic brown color (Fig. 1). After preparation of the dispersions, UV-vis spectroscopy was used to measure the presence of the

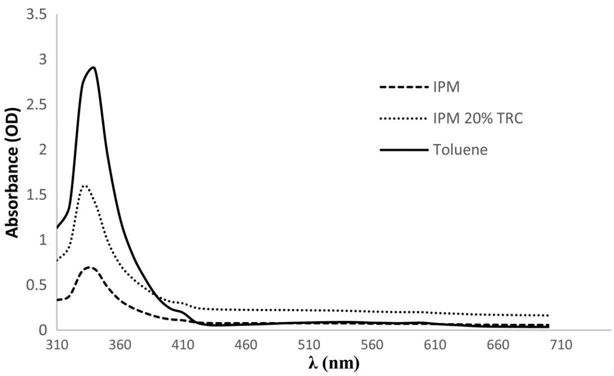

Figure 2. UV-vis spectrum of fullerene C_{60} dispersions prepared with a solution of toluene, with IPM and with IPM with 20% TRC.

fullerenes C_{60} (Fig. 2). All dispersions show a characteristic absorption peak located between 330–340 nm due to the presence of C_{60} molecules [32]. The UV-vis spectrum confirmed the visual observation of the samples, the (darker) solution of IPM with TRC presented larger quantities of the C_{60}. Fullerene C_{60} in toluene was used as control sample for the absorption spectrum.

The poor solubility of fullerene C_{60} in aqueous solutions has captured the attention of researchers. Basically this problem has been overtaken by functionalization [33, 34]. A variety of investigations of well-characterized compounds for potential applications in biomedicine have been conducted in biopharmaceuticals and cosmetics [2, 35–37]. An alternative, simpler, way for fullerene C_{60} application has also been explored using fatty acid esters of glycerol as biocompatible solvents. The solubility of fullerene C_{60} can be effective using vegetable oils [24,38,39]. This prompted us to study C_{60} dispersions with suitable oils for cosmetics/pharma applications: the isopropyl myristate associated with transcutol. IPM presents good spreading properties and is easily absorbed into the skin constituting an excellent substitute for natural oils [40]. The presence of transcutol in the solution of IPM allowed a better dispersion of the fullerene C_{60} due to its powerful solubilization properties. In addition, the nontoxicity and biocompatibility of transcutol with the skin also makes it an attractive penetration enhancer [41, 42].

The quantitative and qualitative permeation of the fullerene C_{60} was investigated through in vitro transdermal perfusion using Franz diffusion cells. Porcine skin was used because presents thickness and absorption rates similar to those of human skin [43–51]. The pig skin was removed from the Franz diffusion cell after the incubation period.

Then, the liquid in donor and receptor compartments was analyzed to measure the fullerene C_{60} concentration in each compartment. For that, a simple LLE method was used. The calibration curve was previously obtained by fullerene C_{60} solutions dissolved in toluene. Thus, fullerene C_{60} that crossed the entire length of the skin until reach the receptor compartment (in the aqueous phase) was extracted to toluene by LLE (using equal volumes: 5 mL). After addition of toluene two immiscible phases were formed. After vigorous agitation the fullerene C_{60} was separated. After separation, the phase containing the fullerene C_{60} was removed and quantified by its UV-vis absorbance at 340 nm. About 10% of fullerene C_{60} remained on top (donor) and 14% of fullerene C_{60} crossed the skin until the receptor compartment. The difference between the detected amount of fullerene C_{60} in donor and in receptor compartment was 76% meaning that fullerene C_{60} was mainly retained into the skin.

The qualitative permeation of the fullerene C_{60} through the intact skin was investigated by transmission electron microscopy (TEM) analysis. The integrity of the skin was monitored and maintained intact to ensure a valid permeation profile of the fullerene C_{60} through the pig skin. Prior to the TEM analysis the skin samples were washed to remove any compounds of the formulation. The samples were frozen at –80°C for later sectioning and mounting in copper grids for TEM visualization. The dispersed fullerene C_{60} was able to cross the intact skin from *stratum corneum* until dermis layer, the inner layer of the skin. The localization and permeation extend of fullerene C_{60} is depicted by TEM analysis in Fig. 3 that clearly show the presence of C_{60} aggregates in the skin sample. This is consistent with the results attained by in vitro permeation profile (quantitative assessment) as well as by molecular dynamics simulations (Fig. 4).

After the experimental evidence on the ability of fullerene C_{60} to cross the skin, molecular dynamics simulations were performed to clarify the mechanism leading to the penetration of the fullerene molecules into the skin. Drug molecules in contact with the skin surface can penetrate by three potential pathways: through the sweat ducts, via the hair follicles and sebaceous glands (collectively called the shunt or appendageal route), or directly across the *stratum corneum* [52]. However, it is generally accepted that as the appendages comprise a fractional area for permeation of approximately 0.1%, the major contribution to steady-state flux of most drugs come from the *stratum corneum*. Our model of the *stratum corneum* is a model of the lipidic membrane. To penetrate through the skin, the molecules have to cross the lipidic membrane, as this membrane occupies the spaces between the corneocytes. Our molecular models show that the fullerene C_{60} has the ability to penetrate the membrane unaided, Fig. 4. It is also possible to observe that for higher concentrations (Fig. 4, B2), the fullerene molecules form aggregates inside the membrane, which is in line with our TEM experiments and previous computer simulations in similar systems [53]. Fullerene aggregates are not present at lower concentrations (Fig. 4, A2).

Full permeation of the fullerene C_{60} throughout the membrane was not observed in our MD (1 μs) simulations. Either the process is kinetically unlikely, or the symmetry conditions in this type of simulations, with periodic boundary conditions lack the driving force necessary to observe the complete permeation as the top layer of the membrane shares the same chemical potential with the bottom layer.

In order to study the complete permeation of C_{60}, the changes in the free energy for a fullerene C_{60} molecule traversing the membrane were computed. After a pulling simulation, represented in Fig. 5, the potential of the mean force across the trajectory was determined through umbrella sampling. On Fig. 6 is depicted the variation of potential of mean force calculated across the trajectory of the pulling simulation of fullerene. It is not easy for fullerene molecules to cross the water layers inside the lipid membrane, and the charged head groups of the lipids, in contact with water could have a major influence in

Eng. Life Sci. **2017**, *17*, 732–738

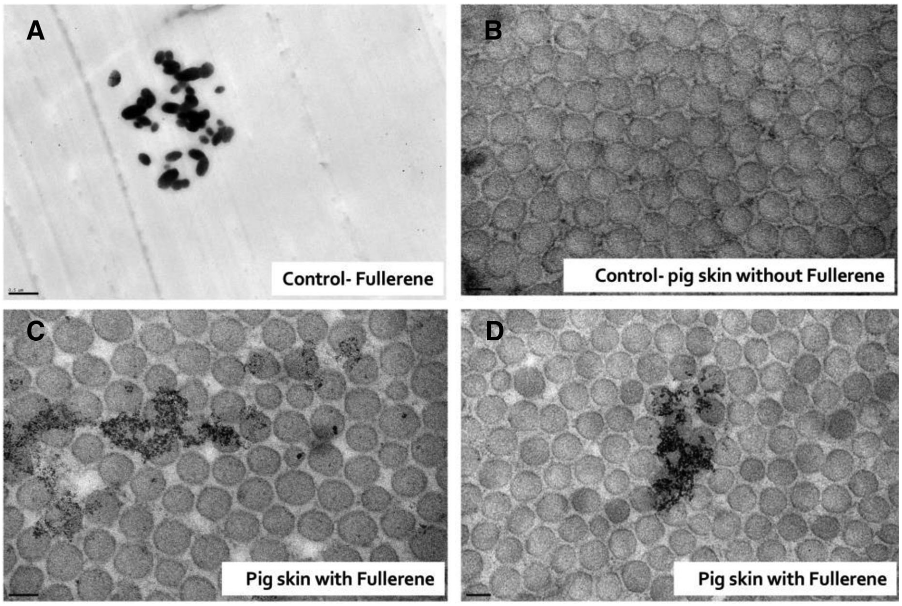

Figure 3. Detection of the fullerene C_{60} into the dermis layer of the pig skin. TEM images of (A) a dispersion solution of fullerene C_{60}; the scale bar represents 500 nm; (B) pig skin in absence of fullerene C_{60}; the scale bar represents 200 nm; (C) and (D) pig skin with fullerene C_{60}; the scale bar represents 100 nm.

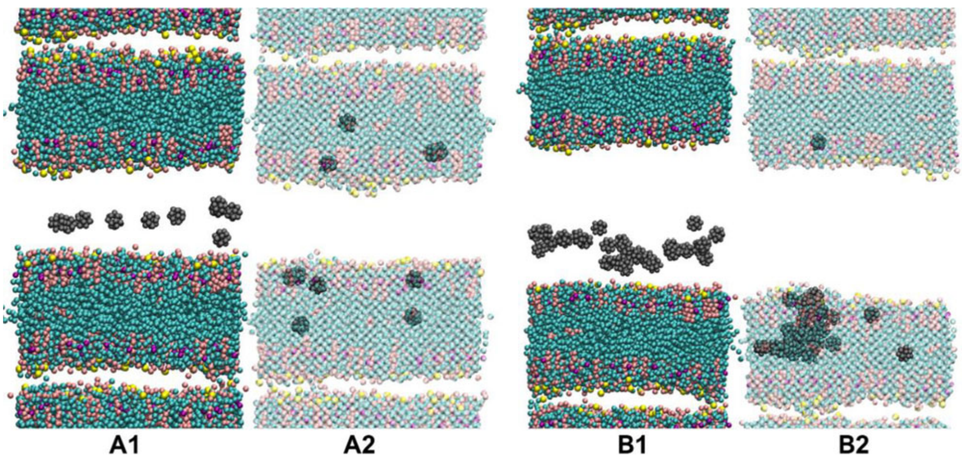

Figure 4. Molecular dynamics snapshots showing fullerene spheres penetrating the lipid membrane of the skin. The water molecules and the ions, filling the empty spaces between lipidic layers, are not showed for clarity. In the pictures A2 and B2 the lipids were made transparent to allow the observation of the fullerene inside the membrane. A – Simulation with 10 fullerene molecules. A1 – Starting point. A2 – after 1 μs of simulation. B – Simulation with 30 fullerene molecules. B1 – Starting point. B2 – after 1 μs of simulation.

this behavior. As previously observed the opening of the lipid membrane has an activation barrier [54] and the fullerenes are stabilized (have negative-free energy) in the apolar, lipid tails, regions.

The membrane model is a small one, with only four lipid bilayers, yet the energetics of a C_{60} molecule on the four bilayers are different and cannot be extrapolated from single bilayer models. In fact, the computed energetics indicate that the penetration of the fullerene into the deeper layers of the skin is a favorable process, as the potential of the mean force value for the second bilayer is almost the double of the value for the first bilayer. In addition, there is a sizeable energy barrier at ζzero that could be an indication that it is energetically difficult to cross the inner water layers inside the skin, but that value could be a consequence of the symmetry of the model. Note also, that this is a highly idealized model and the lipid organizations in the skin may not be as straight as in the simulations allowing for permeation routes that avoid water layers.

4 Concluding remarks

The application of fullerene C_{60} for transdermal delivery was assessed and validated through in vitro tests using pig skin as a model. Fullerene C_{60} was found to be able to cross the intact skin after its dispersion in a solution of fatty acids (IPM with 20% TRC). To ensure the validation and the relevance of the obtained fullerene C_{60} permeation, the integrity of the skin was maintained throughout all experiments. The successful permeation of fullerene C_{60} into the dermis layer was supported by molecular dynamics simulations. These results reveal that a simple formulation using fatty acids can deliver fullerene C_{60} transdermally. From here the use of fullerene C_{60} could be expanded in an easier and greener implementation for the cosmetics/pharmaceutical use. Skin aging and health in general could be improved by the inherent benefits of the antioxidant properties of the fullerene C_{60}. As far as we know there is no cosmetic/pharmaceutical formulation available using fullerene C_{60} in isopropyl myristate

Eng. Life Sci. **2017**, *17*, 732–738

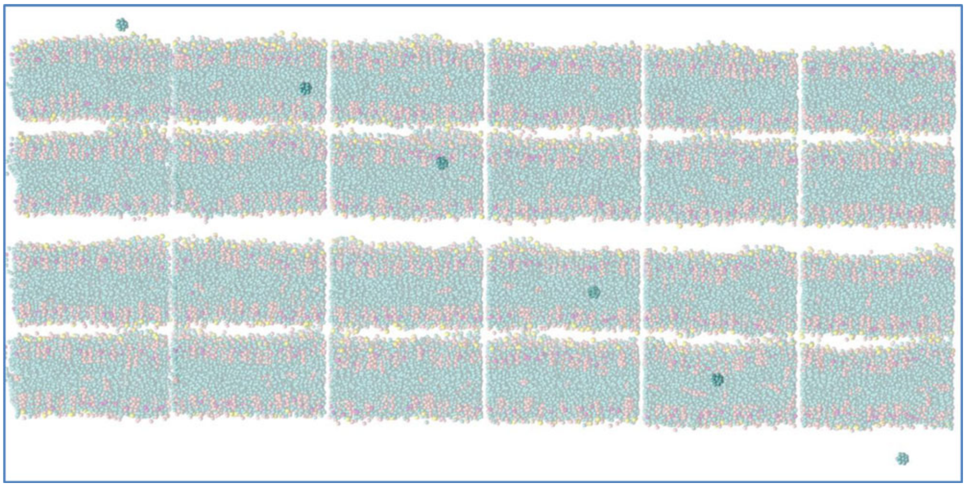

Figure 5. Snapshots of the pulling simulation. The lipids are represented transparent to allow the observation of the fullerene molecule.

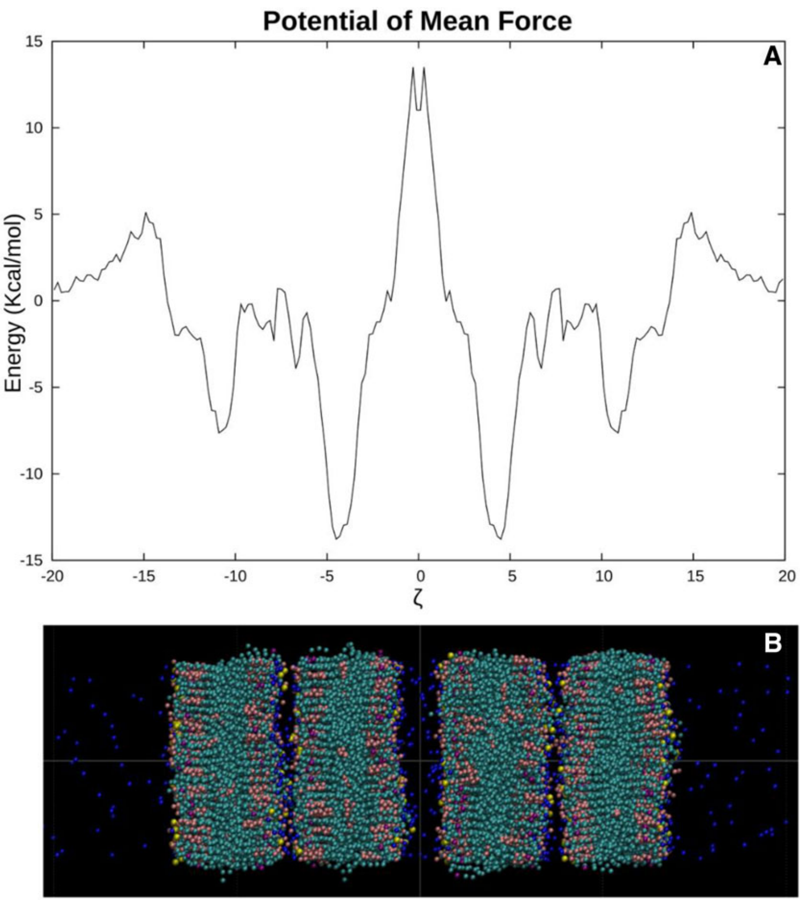

Figure 6. (A) Potential of mean force calculated across the trajectory of the pulling simulation. ζ represents the reaction coordinate defined as the distance between the fullerene molecule center of mass and the middle plane of the membrane. (B) Representation of the membrane model. The membrane is represented on the graph scale for the direct visualization of the reaction coordinate showing that the energy minima are located in the interior of the bilayers.

and/or transcutol. These dispersions make fullerene C_{60} suitable to be delivered transdermally by direct application in the skin without harsh organic solvents or any chemical modification or encapsulation process.

The benefits of antioxidants have been extensively investigated, particularly in general heath (e.g. extending the lifespan) or in skin aging (delaying the normal aging process).

This study was supported by the Portuguese Foundation for Science and Technology (FCT) under the scope of the strategic funding of UID/BIO/04469/2013 unit and COMPETE 2020 (POCI-01-0145-FEDER-006684).). Artur Ribeiro thanks FCT for the SFRH\BPD\98388\2013 grant.

The authors have declared no conflict of interest.

5 References

[1] Kroto, H. W., Heath, J. R., O'Brien, S. C., Curl, R. F. et al., C60: Buckminsterfullerene. *Nature* 1985, *318*, 162–163.

[2] Zhou, Z, Liposome formulation of fullerene-based molecular diagnostic and therapeutic agents. *Pharmaceutics* 2013, *5*, 525–541.

[3] Krusic, P. J., Wasserman, E., Keizer, P. N., Morton, J. R. et al., Radical reactions of C60. *Sciences* 1991, *254*, 1183–1185.

[4] Wang, I. C., Tai, L. A., Lee, D. D., Kanakamma, P. P. et al., C60 and water-soluble fullerene derivatives as antioxidants against radical-initiated lipid peroxidation. *J. Med. Chem.* 1999, *42*, 4614–4620.

[5] Anilkumar, P., Lu, F., Cao, L., Luo, P. G. et al., Fullerenes for applications in biology and medicine. *Curr. Med. Chem.* 2011, *18*, 2045–2059.

[6] Bosi, S., Da Ros, T., Spalluto, G., Prato, M., Fullerene derivatives: An attractive tool for biological applications. *Eur. J. Med. Chem.* 2003, *38*, 913–923.

[7] Lobo, V., Patil, A., Phatak, A., Chandra, N., Free radicals, antioxidants and functional foods: Impact on human health. *Pharmacognosy Rev.* 2010, *4*, 118–126.

[8] Nimse, S. B., Pal, D., Free radicals, natural antioxidants, and their reaction mechanisms. *RSC Adv.* 2015, *5*, 27986–28006.

[9] Dellinger, A., Zhou, Z., Connor, J., Madhankumar, A. B. et al., Application of fullerenes in nanomedicine: An update. *Nanomedicine* 2013, *8*, 1191–1208.

[10] Daroczi, B., Kari, G., McAleer, M. F., Wolf, J. C. et al., In vivo radioprotection by the fullerene nanoparticle DF-1 as assessed in a zebrafish model. *Clin. Cancer. Res.* 2006, *12*, 7086–7091.

[11] Ngan, C. L., Basri, M., Tripathy, M., Abedi Karjiban, R. et al., Skin intervention of fullerene-integrated nanoemulsion in structural and collagen regeneration against skin aging. *Eur. J. Pharm. Sci.* 2015, *70*, 22–28.

[12] Dugan, L. L., Turetsky, D. M., Du, C., Lobner, D. et al., Carboxyfullerenes as neuroprotective agents. *Proc. Natl. Acad. Sci. USA* 1997, *94*, 9434–9439.

[13] Basso, A. S., Frenkel, D., Quintana, F. J., Costa-Pinto, F. A. et al., Reversal of axonal loss and disability in a mouse model of progressive multiple sclerosis. *J. Clin. Invest.* 2008, *118*, 1532–1543.

[14] Gonzalez, K. A., Wilson, L. J., Wu, W., Nancollas, G. H., Synthesis and in vitro characterization of a tissue-selective fullerene: Vectoring C60(OH)16AMBP to mineralized bone. *Biorg. Med. Chem.* 2002, *10*, 1991–1997.

[15] Dellinger, A., Zhou, Z., Lenk, R., MacFarland, D. et al., Fullerene nanomaterials inhibit phorbol myristate acetate-induced inflammation. *Exp. Dermatol.* 2009, *18*, 1079–1081.

[16] Catalán, J., Saiz, J. L., Laynez, J. L., Jagerovic, N. et al., The colors of C60 solutions. *Angewandte Chemie International Edition in English* 1995, *34*, 105–107.

[17] Ruoff, R. S., Tse, D. S., Malhotra, R., Lorents, D. C., Solubility of fullerene (C60) in a variety of solvents. *J. Phys. Chem.* 1993, *97*, 3379–3383.

[18] Makitra, R. G., Pristanskii, R. E., Flyunt, R. I., Solvent Effects on the Solubility of C60 fullerene. *Russ. J. Gen. Chem.* 2003, *73*, 1227-1232.

[19] Kiss, I. Z., Mándi, G., Beck, M. T., Artificial neural network approach to predict the solubility of C60 in various solvents. *J. Phys. Chem. A* 2000, *104*, 8081–8088.

[20] Sayes, C. M., Gobin, A. M., Ausman, K. D., Mendez, J. et al., Nano-C60 cytotoxicity is due to lipid peroxidation. *Biomaterials* 2005, *26*, 7587–7595.

[21] Aschberger, K., Johnston, H. J., Stone, V., Aitken, R. J. et al., Review of fullerene toxicity and exposure—appraisal of a human health risk assessment, based on open literature. *Reg. Toxicol. Pharmacol.* 2010, *58*, 455–473.

[22] Cataldo, F., Encapsulation of C60 fullerene in γ-cyclodextrin: A new concept in the protection of organic substrates and polymers from ozone attack: Kinetic aspects on the reactivity between C60 and O3. *Polym. Degradation Stab.* 2002, *77*, 111–120.

[23] Benn, T. M., Westerhoff, P., Herckes, P., Detection of fullerenes (C60 and C70) in commercial cosmetics. *Environ. Pollut.* 2011, *159*, 1334–1342.

[24] Braun, T., Márk, L., Ohmacht, R., Sharma, U., Olive oil as a biocompatible solvent for pristine C60. *Fullerenes Nanotubes Carbon Nanostruct.* 2007, *15*, 311–314.

[25] Cataldo, F., Braun, T., The solubility of C60 fullerene in long chain fatty acids esters. *Fullerenes Nanotubes Carbon Nanostruct.* 2007, *15*, 331–339.

[26] Cataldo, F., Solubility of fullerenes in fatty acids esters: A new way to deliver in vivo fullerenes. Theoretical calculations and experimental results. In: Cataldo, F., Da Ros, T. (Eds.), *Medicinal Chemistry and Pharmacological Potential of Fullerenes and Carbon Nanotubes.* Springer Netherlands, Dordrecht 2008, pp. 317–335.

[27] Hess, B., Kutzner, C., van der Spoel, D., Lindahl, E. GROMACS 4: Algorithms for highly efficient, load-balanced, and scalable molecular simulation. *J. Chem. Theory Comput.* 2008, *4*, 435–447.

[28] Marrink, S. J., Risselada, H. J., Yefimov, S., Tieleman, D. P. et al., The MARTINI force field: Coarse grained model for biomolecular simulations. *J. Phys. Chem. B* 2007, *111*, 7812–7824.

[29] Hess, B., Bekker, H., Berendsen, H. J. C., Fraaije, J. G. E. M., LINCS: A linear constraint solver for molecular simulations. *J. Comput. Chem.* 1997, *18*, 1463–1472.

[30] Berendsen, H. J. C., Postma, J. P. M., van Gunsteren, W. F., DiNola, A. et al., Molecular dynamics with coupling to an external bath. *J. Chem. Phys.* 1984, *81*, 3684.

[31] Martins, M., Azoia, N. G., Ribeiro, A., Shimanovich, U. et al., In vitro and computational studies of transdermal perfusion of nanoformulations containing a large molecular weight protein. *Colloids Surfaces B* 2013, *108*, 271–278.

[32] Torres, V. M., Posa, M., Srdjenovic, B., Simplício, A. L., Solubilization of fullerene C60 in micellar solutions of different solubilizers. *Colloids Surfaces B* 2011, *82*, 46–53.

[33] He, C.-L., Liu, R., Li, D.-D., Zhu, S.-E. et al., Synthesis and functionalization of [60] fullerene-fused imidazolines. *Organic Lett.* 2013, *15*, 1532–1535.

[34] Afreen, S., Muthoosamy, K., Manickam, S., Hashim, U., Functionalized fullerene (C60) as a potential nanomediator in the fabrication of highly sensitive biosensors. *Biosensors Bioelectronics* 2015, *63*, 354–364.

[35] Gao, J., Wang, H. L., Shreve, A., Iyer, R. Fullerene derivatives induce premature senescence: A new toxicity paradigm or novel biomedical applications. *Toxicol. Appl. Pharmacol.* 2010, *244*, 130–143.

[36] Partha, R., Conyers, J. L., Biomedical applications of functionalized fullerene-based nanomaterials. *Int. J. Nanomed.* 2009, *4*, 261–275.

[37] Benn, T. M., Westerhoff, P., Herckes, P., Detection of fullerenes (C(60) and C(70)) in commercial cosmetics. *Environ. Poll.* 2011, *159*, 1334–1342.

[38] Marcus, Y., Smith, A. L., Korobov, M. V., Mirakyan, A. L. et al., Solubility of C60 fullerene. *J. Phys. Chem. B* 2001, *105*, 2499–2506.

[39] Cataldo, F., Solubility of fullerenes in fatty acids esters: A new way to deliver in vivo fullerenes. Theoretical calculations and experimental results. In: Cataldo, F., Da Ros, T. (Eds.), *Medicinal chemistry and pharmacological potential of fullerenes and carbon nanotubes*. Springer Netherlands, Dordrecht 2008, pp. 317–335.

[40] Sato, K., Sugibayashi, K., Morimoto, Y., Effect and mode of action of aliphatic esters on the in vitro skin permeation of nicorandil. *Int. J. Pharm.* 1988, *43*, 31–40.

[41] Mura, P., Faucci, M. T., Bramanti, G., Corti, P. Evaluation of transcutol as a clonazepam transdermal permeation enhancer from hydrophilic gel formulations. *Eur. J. Pharma. Sci.* 2000, *9*, 365–372.

[42] Godwin, D. A., Kim, N.-H., Felton, L. A., Influence of Transcutol® CG on the skin accumulation and transdermal permeation of ultraviolet absorbers. *Eur. J. Pharm. Biopharm.* 2002, *53*, 23–27.

[43] Marzulli, F., Maibach, H. I., Relevance of animal models: the hexachlorophene story, In: Maibach, H. I. (Ed.), *Animal models in dermatology*. Churchill Livingstone. Edinburgh 1975, pp. 156–167.

[44] Bronaugh, R. L., Stewart, R. F., Congdon, E. R., Methods for in vitro percutaneous absorption studies II. Animal models for human skin. *Toxicol. Appl. Pharmacol.* 1982, *62*, 481–488.

[45] Haigh, J. M., Smith, E. W., The selection and use of natural and synthetic membranes for in vitro diffusion experiments. *Eur. J. Pharm. Sci.* 1994, *2*, 311–330.

[46] Morris, G. M., Hopewell, J. W., Epidermal cell kinetics of the pig: A review. *Cell Prolif.* 1990, *23*, 271–282.

[47] Sullivan, T. P., Eaglstein, W. H., Davis, S. C., Mertz, P., The pig as a model for human wound healing. *Wound Repair Regen.* 2001, *9*, 66–76.

[48] Harunari, N., Zhu, K. Q., Armendariz, R. T., Deubner, H. et al., Histology of the thick scar on the female, red Duroc pig: Final similarities to human hypertrophic scar. *Burns* 2006, *32*, 669–677.

[49] Gallo, S. A., Sen, A., Hensen, M. L., Hui, S. W. Time-dependent ultrastructural changes to porcine stratum corneum following an electric pulse. *BpJ.* 1999, *76*, 2824–2832.

[50] Holbrook, K. A., Odland, G. F., Regional differences in the thickness (cell layers) of the human stratum corneum: An ultrastructural analysis. *J. Invest. Dermatol.* 1974, *62*, 415–422.

[51] Wester, R. C., Melendres, J., Sedik, L., Maibach, H. et al., Percutaneous absorption of salicylic acid, theophylline, 2,4-dimethylamine, diethyl hexyl phthalic acid, andp-aminobenzoic acid in the isolated perfused porcine skin flap compared to manin vivo. *Toxicol. Appl. Pharmacol.* 1998, *151*, 159–165.

[52] Benson, H., Transdermal drug delivery: Penetration enhancement techniques. *Curr. Drug Delivery* 2005, *2*, 23–33.

[53] Höfinger, S., Melle-Franco, M., Gallo, T., Cantelli, A. et al., A computational analysis of the insertion of carbon nanotubes into cellular membranes. *Biomaterials* 2011, *32*, 7079–7085.

[54] Bedrov, D., Smith, G. D., Davande, H., Li, L. Passive transport of C60 fullerenes through a lipid membrane: A molecular dynamics simulation study. *J. Phys. Chem. B* 2008, *112*, 2078–2084.